Supporting Information

BIAN-paraphenylene Type Condensation Copolymer Binder for Ultra-long cyclable Lithium-Ion Rechargeable Battery

*Agman Gupta, Rajashekar Badam, Aniruddha Nag, Tatsuo Kaneko, and Noriyoshi Matsumi**

Graduate School of Advanced Science and Technology, Japan Advanced Institute of Science and Technology (JAIST), 1-1 Asahidai, Nomi, Ishikawa 923-1292, Japan.
matsumi@jaist.ac.jp

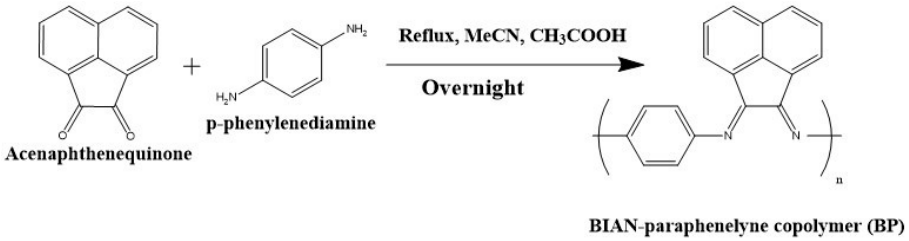

Figure S1: Synthetic scheme of the BP-copolymer

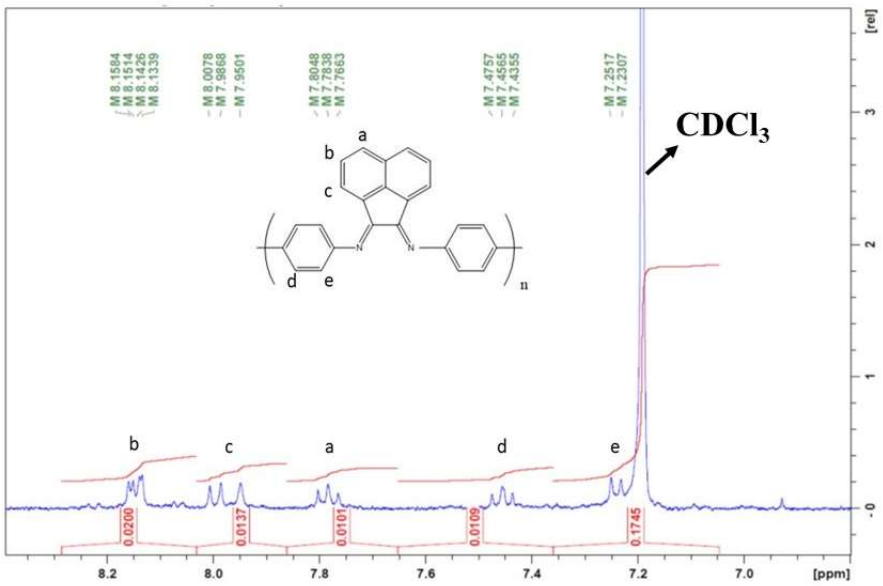

Figure S2: ^{1}H-NMR spectrum of BP-copolymer

Supporting Information

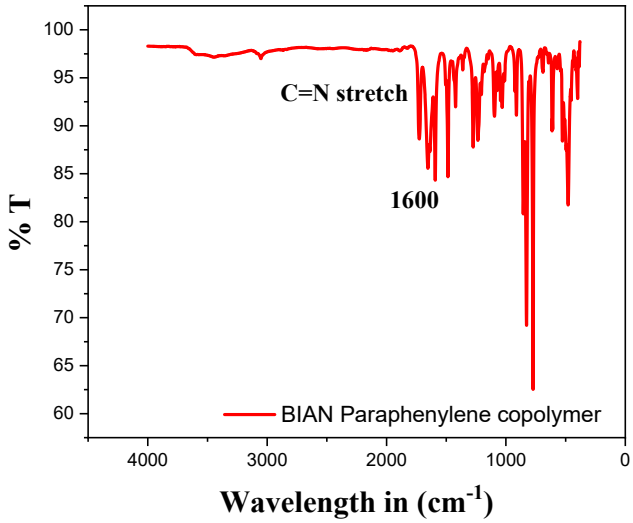

Figure S3: FT-IR spectrum of the BP-copolymer

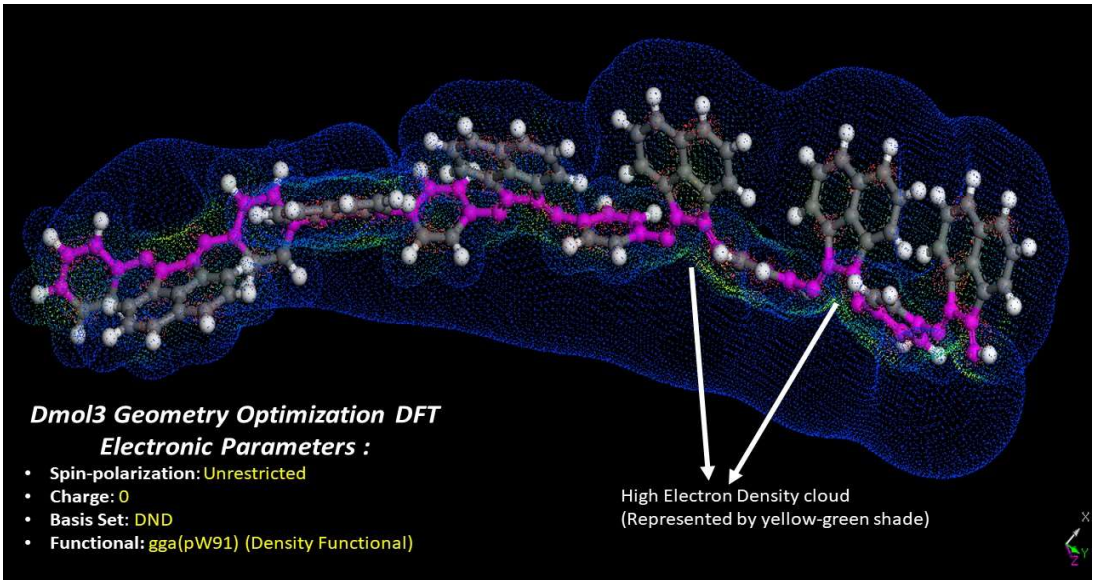

Figure S4: Optimized Structure of the BP-copolymer obtained after DFT calculations

Supporting Information

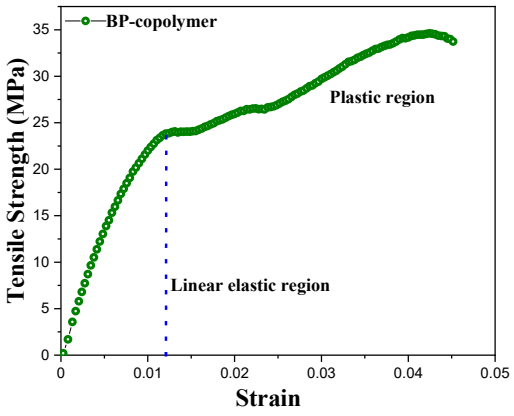

Figure S5: Tensile curve for BP-copolymer binder at 25 ° C with a draw ratio of 3 mm/min.

Samples	Tensile Strength (MPa)	Young's Modulus (GPa)	Strain (%)
BP-copolymer	34 ± (1.2)	1.1 ± (0.7)	4.4 ± (0.6)
PVDF[1]	22 ± (2.9)	0.35 ± (0.04)	2.4 ± (1.0)

Table S1: Tensile properties of BP-copolymer and PVDF

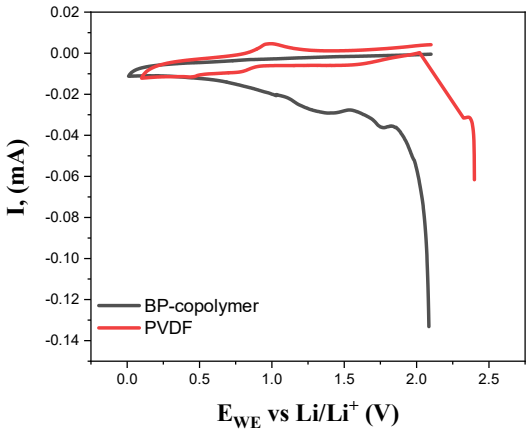

Figure S6: The first cycle CV of pure BP-copolymer and PVDF polymer films on the current collector with respect to lithium electrode in 1M $LiPF_6$ in (1:1) v/v EC:DEC electrolyte.

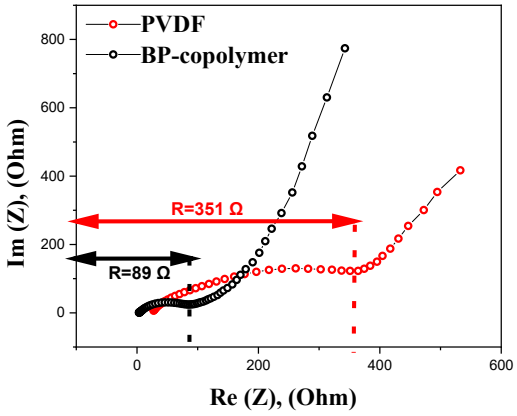

Figure S7: Nyquist spectrum of anodic half-cells having electrodes with pure binder coating (without graphite and acetylene black)

$$R = \rho \frac{l}{A} \qquad (1)$$

In equation 1, R is the resistance in ohm (Ω), l is the length in meter (m) of the specimen, A is the cross-sectional area (m^2) of the specimen, and ρ the resistivity (Ωm). The conductivity σ (Ω^{-1} m^{-1})of a material is the inverse of its resistivity as shown in equation 2.

$$\sigma = \frac{1}{\rho} \qquad (2)$$

Material	Area of the electrode (A)	Thickness of the electrode (L)	Resistance	Conductivity
BP-copolymer	1.77×10^{-4} m^{-2}	60 µm	89 Ω	3.80×10^{-3} Ω^{-1} m^{-1}
PVDF	1.77×10^{-4} m^{-2}	56 µm	351 Ω	9.01×10^{-4} Ω^{-1} m^{-1}

Table S2: Parameters associated with the conductivity measurement of BP and PVDF binders.

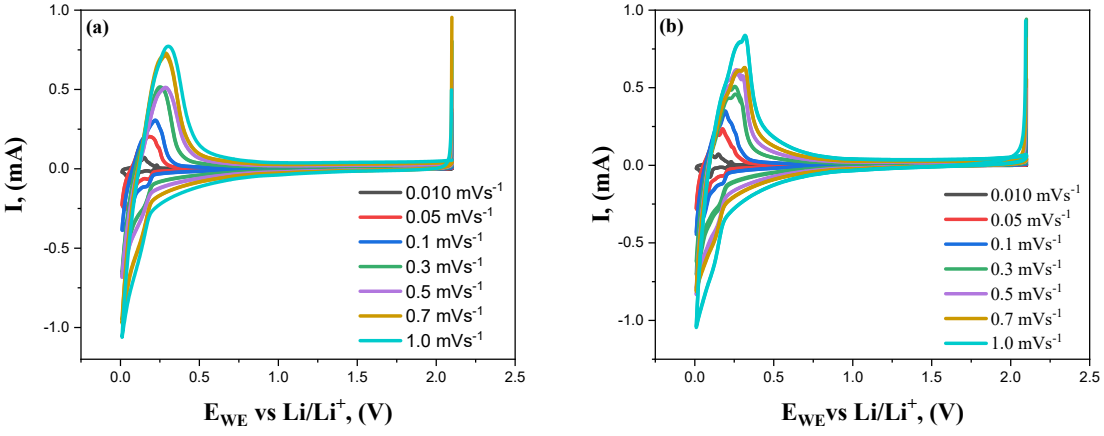

Figure S8: CV at varying scan rates for the graphite electrode with (a) BP-copolymer, and (b) PVDF binders in 1.0 M $LiPF_6$ in (1:1) (v/v) EC:DEC

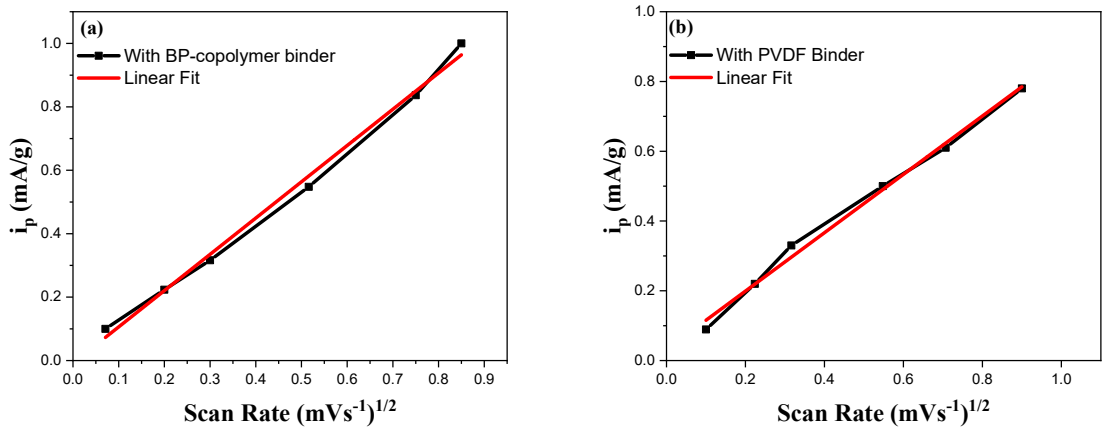

Figure S9: Plot of peak current vs the square root of scan rates (a) BP-copolymer, (b) PVDF

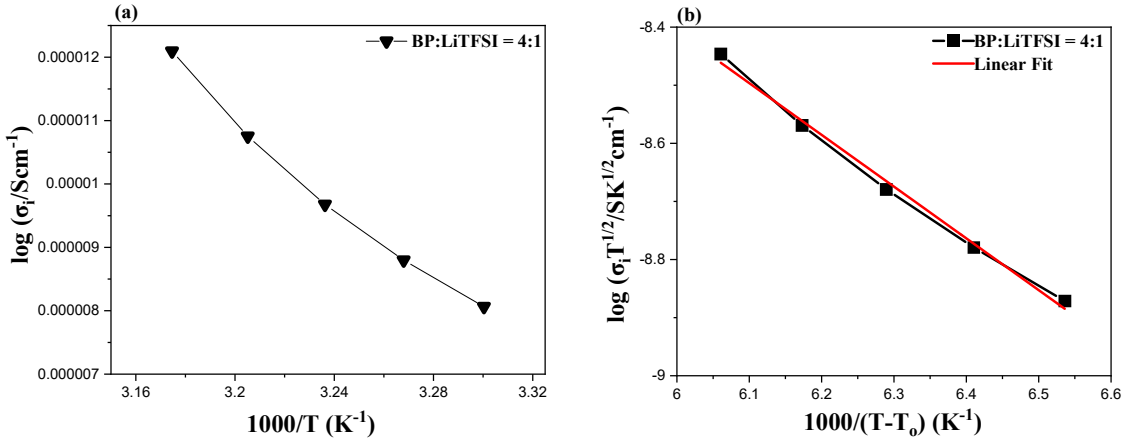

Figure S10: (a) Arrhenius plot of BP-copolymer with LiTFSI (Temperature dependence of the ionic conductivity) and (b) VFT plots of the BP-copolymer with LiTFSI

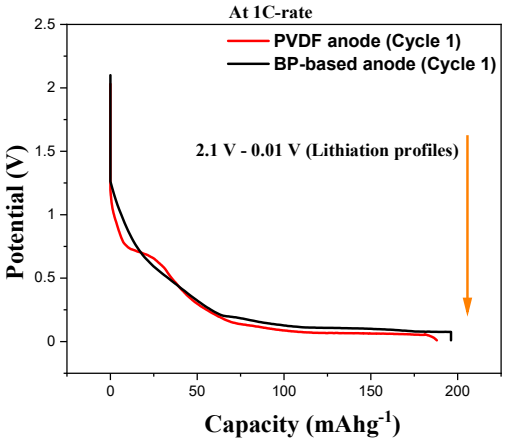

Figure S 11: Comparison between the 1st galvanostatic lithiation cycles of PVDF and BP binder-based anodic half-cells in the potential window 0.01 V – 2.1 V vs Li/Li^+

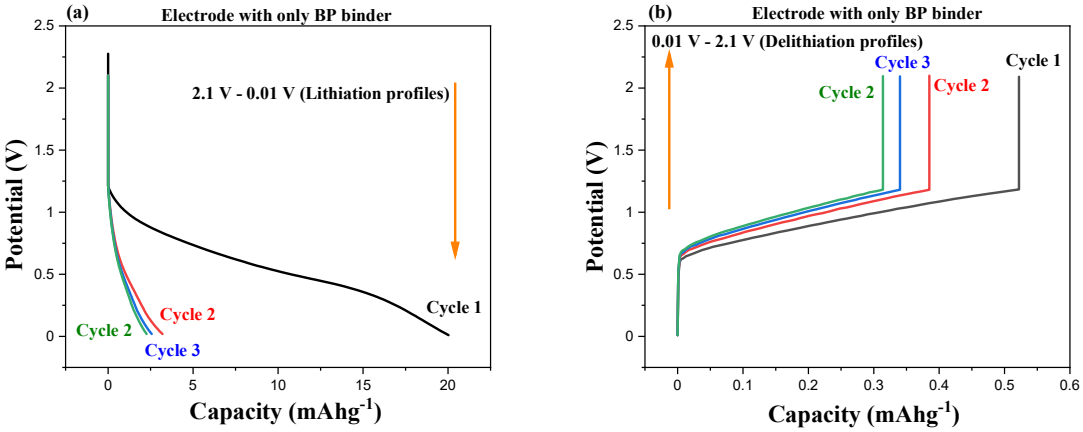

Figure S12: Galvanostatic cycling profiles of the electrode with only BP binder (without graphite and conductive additive) in the potential window 0.01 V – 2.1 V vs Li/Li^+ (a) lithiation half-cycle profiles for cycle 1, cycle 2, and cycle, and (b) delithation half-cycle profiles for cycle 1, cycle 2 and cycle 3, respectively.

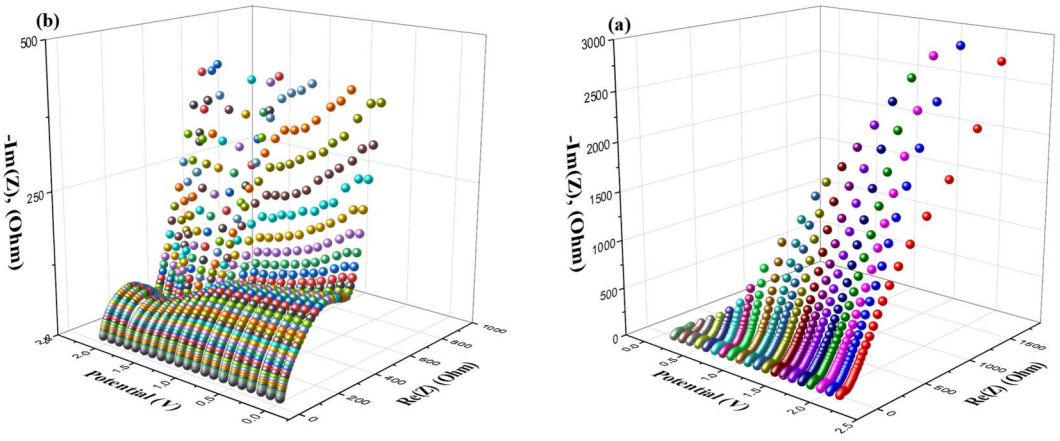

Figure S13: DEIS profiles during the delithiation of the anodic half-cells with (a) BP-copolymer (after 1735 cycles at 1C), (b) PVDF (after 525 cycles at 1C)

Supporting Information

R_E	R_{PC}	R_{SEI}	R_{CT}	χ^2	Circuit	Potential (V)
0.029	1.822	62.53	5.18E+01	5.00E-04	R(L)(QR)(QR)(QR)(QW)	0.01
2.391	15.54	66.48	5.98E-05	4.73E-05	R(L)(QR)(QR)(QR)(QW)	0.11
2.566	49.31	61.19	3.99E+01	1.18E-05	R(L)(QR)(QR)(QR)(QW)	0.21
2.852	704.2	2.529	7.36E+01	2.07E-05	R(L)(QR)(QR)(QR)(QW)	0.32
2.55	61.02	91.19	5.51E+01	1.73E-05	R(L)(QR)(QR)(QR)(QW)	0.42
2.87	63.15	58.77	4.74E+01	4.18E-05	R(L)(QR)(QR)(QR)(QW)	0.52
2.42	540.9	43.19	2.91E+01	1.89E-05	R(L)(QR)(QR)(QR)(QW)	0.63
1.505	173.9	0.9606	6.09E+01	4.12E-05	R(L)(QR)(QR)(QR)(QW)	0.74
0.7	1.75	59.18	496	2.91E-05	R(L)(QR)(QR)(QR)(QW)	0.84
2.44	5.94	56.97	1.57E+04	3.24E-05	R(L)(QR)(QR)(QR)(QW)	0.95
3.04	2.256	65.33	4.28E+02	3.85E-05	R(L)(QR)(QR)(QR)(QW)	1.05
2.97	2.222	63.9	4.32E+02	4.52E-05	R(L)(QR)(QR)(QR)(QW)	1.15
0.3068	2.18	49.99	1.12E+07	9.24E-05	R(L)(QR)(QR)(QR)(QW)	1.26
2.201	8.731	1390	34.36	1.90E-04	R(L)(CR)(QR)(CR)(QW)	1.36
2.423	2.55E+02	322.8	53.21	3.20E-05	R(L)(QR)(QR)(QR)(QW)	1.47
2.54	344.1	49.35	127.5	3.05E-05	R(L)(QR)(QR)(QR)(QW)	1.57
2.544	2096	216.1	49.93	3.51E-05	R(L)(QR)(QR)(QR)(QW)	1.68
2.75	3.13E+11	0.03	45.48	6.79E-05	R(L)(QR)(QR)(QR)(QW)	1.78
2.57	2.79E+04	19.67	42.71	3.00E-05	R(L)(QR)(QR)(QR)(QW)	1.89
2.847	25.81	5338	659.2	5.8×10^{-4}	R(QR)(CR)(QR)(RW)	1.99
2.957	2.162	53.75	3628	0.0007	R(QR)(CR)(QR)(RW)	2.10

Table S3: - DEIS circuit fitting parameters during charging with BP-copolymer as a binder

R_E	R_{PC}	R_{SEI}	R_{CT}	χ^2	Circuit	Potential (V)
2.4	3.62	2.57E+04	126.73	1.00E-04	R(L)(QR)(QR)(QR)(QW)	0.01
2.7	81.38	1.19E+13	200.65	9.00E-05	R(L)(QR)(QR)(QR)(QW)	0.11
1.31	131.7	66.42	400.8	3.00E-04	R(L)(QR)(QR)(QR)(QW)	0.21
2.12	3.46E+04	72.34	13.78	2.69E-05	R(L)(QR)(QR)(QR)(QW)	0.32
2.26	73.25	137.9	100.1	2.23E-05	R(L)(QR)(QR)(QR)(QW)	0.42
2.4	0.87	101	65.86	2.12E-05	R(L)(QR)(QR)(QR)(QW)	0.52
2.65	72.19	91.2	49.68	1.90E-05	R(L)(QR)(QR)(QR)(QW)	0.63
1.8	17.93	57.94	27.89	2.38E-05	R(L)(QR)(QR)(QR)(QW)	0.74
0.12	1.89	68.11	198.24	3.20E-05	R(L)(QR)(QR)(QR)(QW)	0.84
2.15	188.9	66.43	347.87	3.52E-05	R(L)(QR)(QR)(QR)(QW)	0.95
2.53	6.79	76.56	231.97	4.60E-05	R(L)(QR)(QR)(QR)(QW)	1.05
2.51	1.065	69.89	87.31	4.70E-05	R(L)(QR)(QR)(QR)(QW)	1.15
2.15	66.3	9307	100.96	1.00E-04	R(L)(QR)(QR)(QR)(QW)	1.26
0.82	1.36	6527	234.21	1.00E-04	R(L)(QR)(QR)(QR)(QW)	1.36
2.92	4.22E+00	278.3	1000.24	9.50E-05	R(L)(QR)(QR)(QR)(QW)	1.47
2.19	6.41E+01	1.01E+04	220.1	6.03E-05	R(L)(QR)(CR)(QR)(CW)	1.57
2.81	1.80E+02	3.73E+01	589	1.00E-04	R(L)(QR)(CR)(QR)(QW)	1.68
2.23	1.06E+03	31.01	119	1.00E-04	R(L)(QR)(CR)(QR)(CW)	1.78
2.47	6.00E+01	253.7	261.9	9.58E-05	R(L)(QR)(QR)(QR)(QW)	1.89
2.17	60.97	7976	320.89	0.0001	R(L)(QR)(QR)(QR)(CW)	1.99
2.81	5865	95.29	300.1	0.0002	R(L)(QR)(QR)(CR)(QW)	2.10

Table S4: - DEIS circuit fitting parameters during charging with PVDF as a binder

Supporting Information

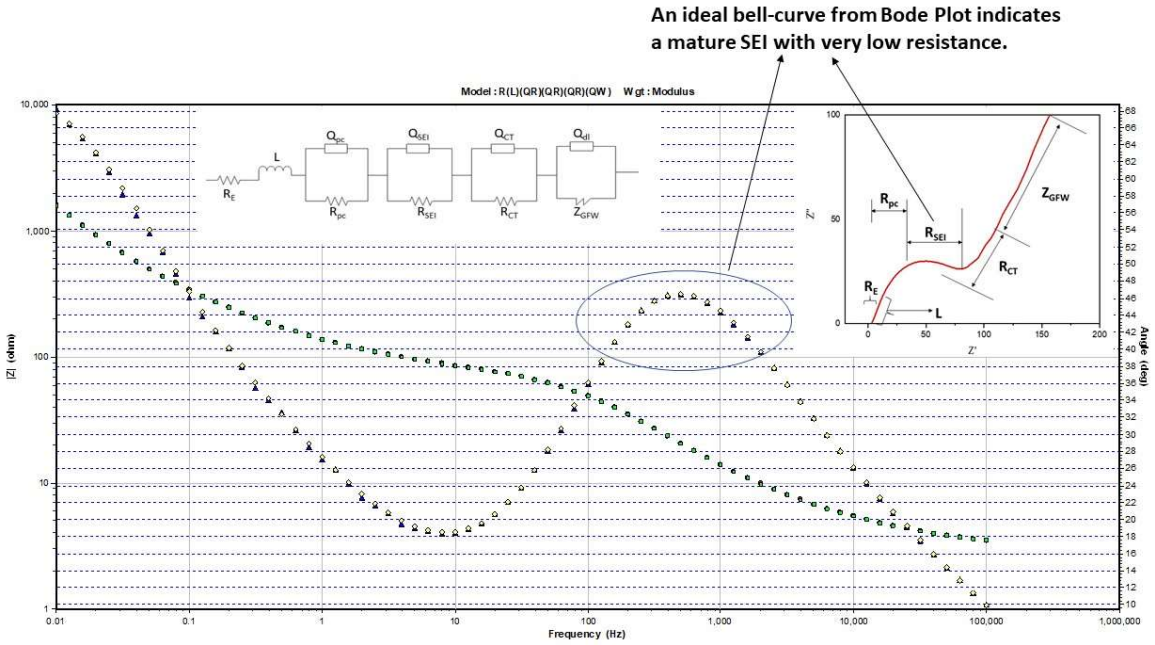

Figure S14: An EECM fit representative Bode's plot during lithiation in case of the BP-copolymer showing various interfaces.

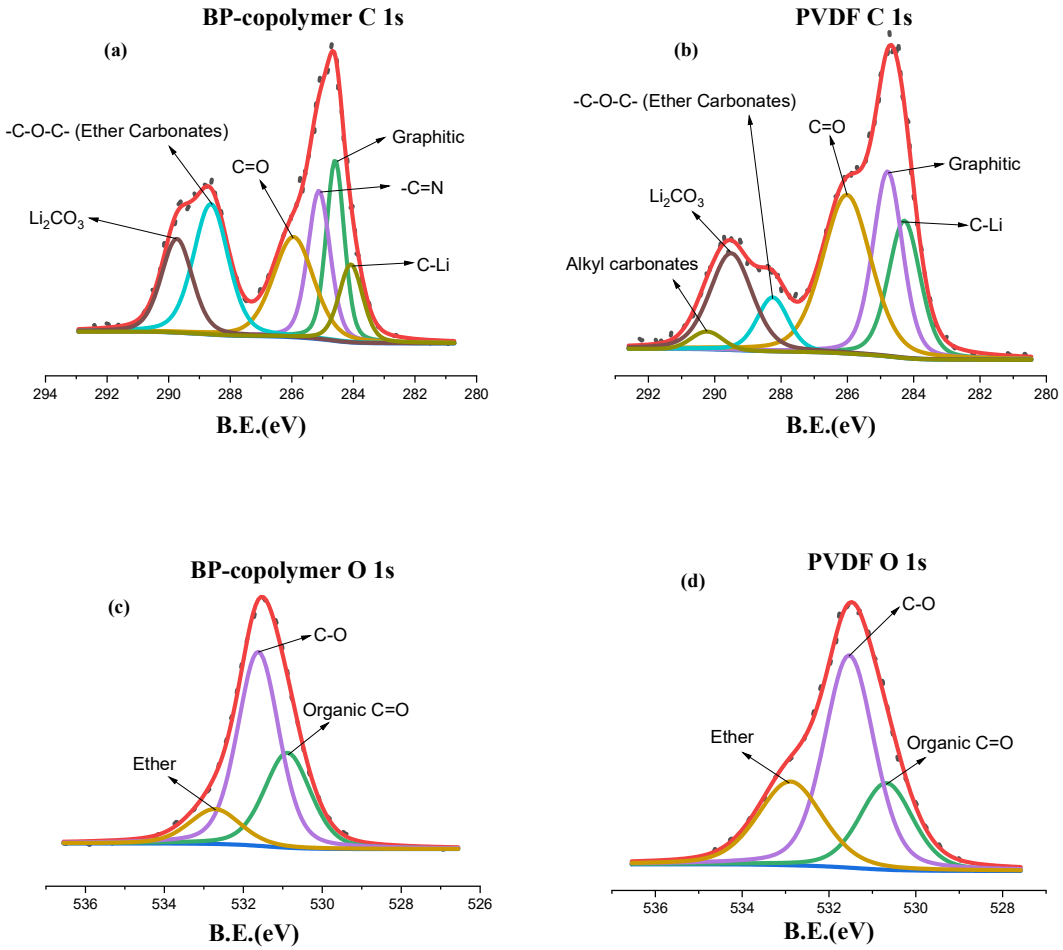

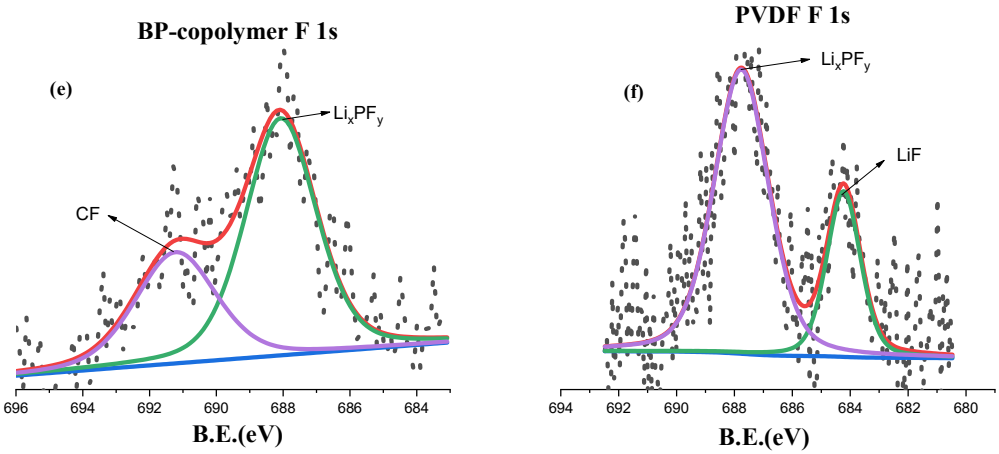

Figure S15: The XPS spectra (a), (c), and (e) for the BP-copolymer binder based anode for C 1s, O 1s, and F 1s respectively, and (b), (d), and (f) for the PVDF binder based anode for C 1s, O 1s and F 1s, respectively, with the respective SEI components.

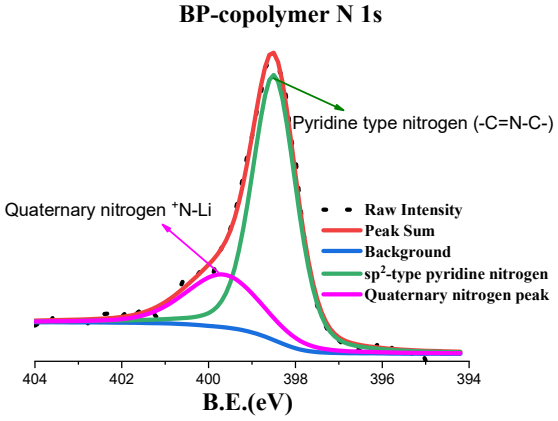

Figure S16: The XPS spectrum of N 1s component of diimine framework of the BP binder-based anode cycled for 1735 cycles.

(a) C 1s (BP-copolymer and PVDF)

Component	BP-copolymer (eV)	% area under the curve	PVDF (eV)	% area under the curve
C-Li	284.08	9.26	284.03	18.35
Graphite	284.6	16.35	284.62	23.37
-C=N	285.11	16.58	-	-
C=O	285.94	20.38	285.82	30.92
C-O-C (ether carbonates)	288.63	22.79	288.03	8.16
Lithium carbonates (Li_2CO_3)	289.73	14.61	289.28	15.34
Alkyl carbonates (R-OCO_2-Li)	-	-	289.93	3.85

(b) O 1s (BP-copolymer and PVDF)

Component	BP-copolymer (eV)	% area under the curve	PVDF (eV)	% area under the curve
C=O (organic species)	530.88	30.82	530.68	22.39
C-O	531.61	56.67	531.52	51.34
Ether	532.72	12.49	532.89	26.25

(c) F 1s (BP-copolymer and PVDF)

Component	BP-copolymer (eV)	% area under the curve	PVDF (eV)	% area under the curve
CF	691.13	34.71		
LiF	-	-	684.32	26.59
Li_xPF_y	687.98	65.28	687.85	73.4

(d) N 1s (BP-copolymer)

Component	BP-copolymer (eV)	% area under the curve
Pyridinic Type	398.59	74.5
Li doped N	399.75	25.49

Table S5 (a), (b), and (c): The binding energy values and corresponding % area under the curve corresponding to C 1s, O 1s, and F 1s for BP-copolymer and PVDF based electrodes. **(d)** corresponding to N 1s for BP-copolymer.

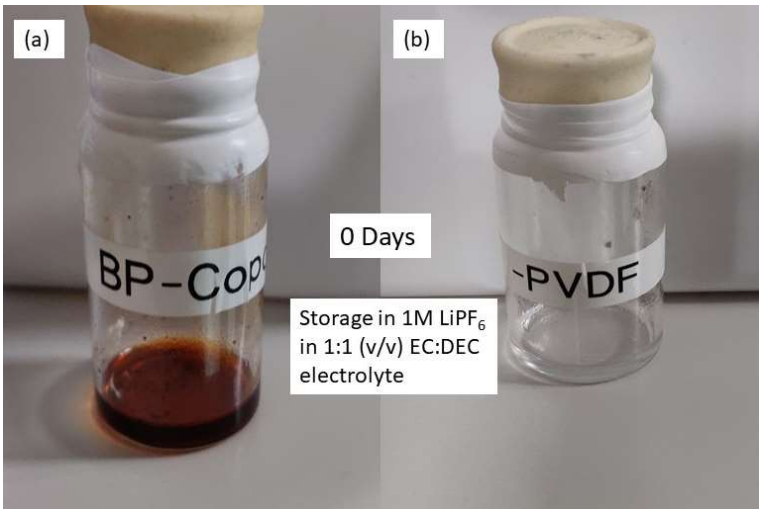

Figure S17: The observation on storage (0 days) in 1M $LiPF_6$ in (1:1) v/v EC:DEC electrolyte (a) BP-copolymer, and (b) PVDF

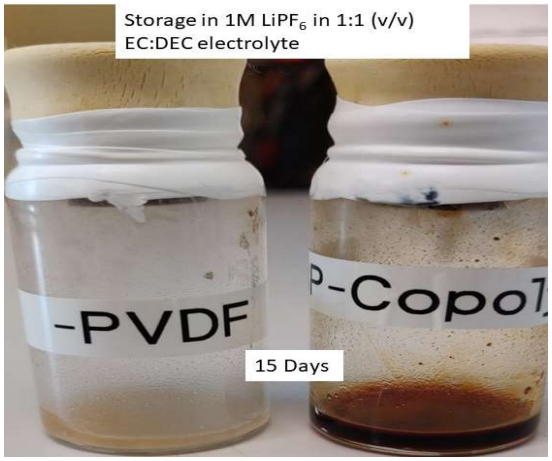

Figure S18: The observation on storage (15 days) in 1M $LiPF_6$ in (1:1) v/v EC:DEC electrolyte of both the binders.

Type of Binder	Active Material (wt %)	Conductive additive (wt %)	Binder content (wt %)	Electrode specification	Specific Capacity	Reference
Cellulose-type binder: CMC	80	10	10	2.25 mg cm^{-3}	200 ($mAhg^{-1}$) at 1C (50 cycles)	2
Natural cellulose	90	5	5	3.0 mg cm^{2}	140 ($mAhg^{-1}$) at 1C-rate (140 cycles)	3
Polyurethane(PU) /carboxymethylcellulose (CMC)	93	4	3	-	130 ($mAhg^{-1}$) at (1C-rate) for 120 cycles	4
Composite-type binder PVDF-PMMA	83	5	12	3.0 mg cm^{-2}	100 ($mAhg^{-1}$) at (1C-rate) for 200 cycles	5
polyVC	80	10	10		180 ($mAhg^{-1}$) at 1C rate for 50 cycles	6
AMMA	95		5	1.27 mg cm^{-2}	200 $mAhg^{-1}$ (0.3 mA cm^{-2}) for 300 cycles	7
Conductive-Type binder PAAX (X=Li, Na, and K)	80	10	10	1.5 mg cm^{-2}	140 $mAhg^{-1}$ at 1C rate for 200 cycles	8
Li-PIMA	90		10	-	320 $mAhg^{-1}$ at 0.1C for 200 cycles	9
This work (BP-copolymer)	80	10	10	1.12 mg cm^{-2}	260 $mAhg^{-1}$ at 1C for 1735 cycles	

Table S6: The comparison of BP binder-based anode's performance with other reported binders in the literature based on the composition of the prepared electrode (contents like active material, conductive additive, and binder).

Type of Binder	Current Rate	Specific Capacity $mAhg^{-1}$	Reference
Na-CMC	0.1C	300	10
	0.5C	180	
	1C	98	
Chitosan	0.1C	103	11
	0.5C	97.5	
	1C	95	
Natural Cellulose	0.1C	155	3
	0.5C	140	
	1C	125	
PolyVC	0.04C	300	6
	0.1C	260	
	1C	220	
PVDF-PMMA	1C	127	5
	2C	123	
	3C	121	
Guar Gum	0.1C	360	10
	0.5C	150	
	1C	75	
CP-CMC	0.1C	103	12
	0.5C	120	
	1C	115	
This work (BP-copolymer)	0.1C	270	
	1C	260	

Table S7: The comparison of cycling performance BP-binder based anodic half-cell at different current-rates with other aqueous binders reported in the literature for the graphite anode.

1. Rath, S. K.; Dubey, S.; Kumar, G. S.; Kumar, S.; Patra, A. K.; Bahadur, J.; Singh, A. K.; Harikrishnan, G.; Patro, T. U., Multi-walled CNT-induced phase behaviour of poly(vinylidene fluoride) and its electro-mechanical properties. *Journal of Materials Science* **2014,** *49* (1), 103-113.

2. Lee, J.-H.; Paik, U.; Hackley, V. A.; Choi, Y.-M., Effect of poly(acrylic acid) on adhesion strength and electrochemical performance of natural graphite negative electrode for lithium-ion batteries. *J Power Sources* **2006,** *161* (1), 612-616.

3. Jeong, S. S.; Böckenfeld, N.; Balducci, A.; Winter, M.; Passerini, S., Natural cellulose as binder for lithium battery electrodes. *J Power Sources* **2012,** *199*, 331-335.

4. Loeffler, N.; Kopel, T.; Kim, G.-T.; Passerini, S., Polyurethane Binder for Aqueous Processing of Li-Ion Battery Electrodes. *Journal of The Electrochemical Society* **2015,** *162* (14), A2692-A2698.

5. Wang, Y.; Zheng, H.; Qu, Q.; Zhang, L.; Battaglia, V. S.; Zheng, H., Enhancing electrochemical properties of graphite anode by using poly(methylmethacrylate)–poly(vinylidene fluoride) composite binder. *Carbon* **2015,** *92*, 318-326.

6. Zhao, H.; Zhou, X.; Park, S.-J.; Shi, F.; Fu, Y.; Ling, M.; Yuca, N.; Battaglia, V.; Liu, G., A polymerized vinylene carbonate anode binder enhances performance of lithium-ion batteries. *J Power Sources* **2014,** *263*, 288-295.

7. Zhang, S. S.; Jow, T. R., Study of poly(acrylonitrile-methyl methacrylate) as binder for graphite anode and LiMn2O4 cathode of Li-ion batteries. *J Power Sources* **2002,** *109* (2), 422-426.

8. Chong, J.; Xun, S.; Zheng, H.; Song, X.; Liu, G.; Ridgway, P.; Wang, J. Q.; Battaglia, V. S., A comparative study of polyacrylic acid and poly(vinylidene difluoride) binders for spherical natural graphite/LiFePO4 electrodes and cells. *J Power Sources* **2011,** *196* (18), 7707-7714.

9. Huang, S.; Ren, J.; Liu, R.; Yue, M.; Huang, Y.; Yuan, G., Enhanced electrochemical properties of a natural graphite anode using a promising crosslinked ionomer binder in Li-ion batteries. *New Journal of Chemistry* **2017,** *41* (20), 11759-11765.

10. Cuesta, N.; Ramos, A.; Cameán, I.; Antuña, C.; García, A. B., Hydrocolloids as binders for graphite anodes of lithium-ion batteries. *Electrochimica Acta* **2015,** *155*, 140-147.

11. Chai, L.; Qu, Q.; Zhang, L.; Shen, M.; Zhang, L.; Zheng, H., Chitosan, a new and environmental benign electrode binder for use with graphite anode in lithium-ion batteries. *Electrochimica Acta* **2013,** *105*, 378-383.

12. Kuenzel, M.; Choi, H.; Wu, F.; Kazzazi, A.; Axmann, P.; Wohlfahrt-Mehrens, M.; Bresser, D.; Passerini, S., Co-Crosslinked Water-Soluble Biopolymers as a Binder for High-Voltage LiNi0.5Mn1.5O4|Graphite Lithium-Ion Full Cells. *ChemSusChem* **2020,** *13* (10), 2650-2660.